United Nations Human Space Technology Initiative (UN-HSTI)
Drop Tower Experiment Series (DropTES), 2016

Final Experiment Report:

Behavior of a Reduced-Scale Robotic Arm Manipulator under Microgravity Conditions

Prepared by:

Nicole Chaves Jiménez
Ernesto Corrales Corrales
Moacir Fonseca Becker
Carlos Mayorga Espinoza

Advisor: Renato Rimolo-Donadio

Institutions:
    Instituto Tecnológico de Costa Rica (ITCR), Universidad de Costa Rica (UCR).

April 30, 2017

I. Introduction

In this report, the activities carried out during the Drop Tower Experiment Series 2016 are documented. The final prototype design, experiment setup and execution are addressed in this document.

The general objective of the work was to design and implement an experiment in microgravity to analyze the influence of torsion, inertial, and reactive forces on a scaled robotic system, which is on a rotating, non-inertial frame of reference. For this experiment, the robotic manipulator was designed within the considerations and requirements of the *Drop Tower* at the Cener of Applied Space Technology and Microgravity (ZARM). The implementation of the robotic manipulator prototype was carried out and then adapted to the drop tower chamber with centrifuge. With a predefined movement sequence, measurements of forces on the arm were carried out by means of load cell sensors and an inertial measurement unit (IMU), both in microgravity conditions and normal earth conditions. During the experiment series, four drops were successfully completed, gathering information from sensors and cameras recording the experiments. The results were analyzed and compared with respect to theoretical expectations and a conference paper publication was prepared, targeting a submission to the International Aeronautic Congress 2017.

II. Design of the Scaled Robotic Manipulator

The experiment consists of a small, articulated robotic manipulator, which was attached on-board to a reduced-gravity centrifuge (rotating platform). The setup consists of a 3 degree of freedom (DoF) manipulator arm, mounted on an aluminum platform which is attached to the rotating base plate of the centrifuge. Through this experiment, the effect of forces over the end effector and base of the robot was studied and compared with simplified analytical models.

Together with this document, the design drawings are provided (see link in Appendix C). Figures 1 and 2 are an extract of the design files, where the view of the setup with the two arms and a detail of a single arm are shown, respectively. With respect to the preliminary designs, the mechanical model suffered modifications to simplify the fabrication process and to adapt it to the actual geometry of the motors and other electronics components bought. The electronic control was placed on top of the plate, which is a more convenient location for the experiment setup at the cabin.
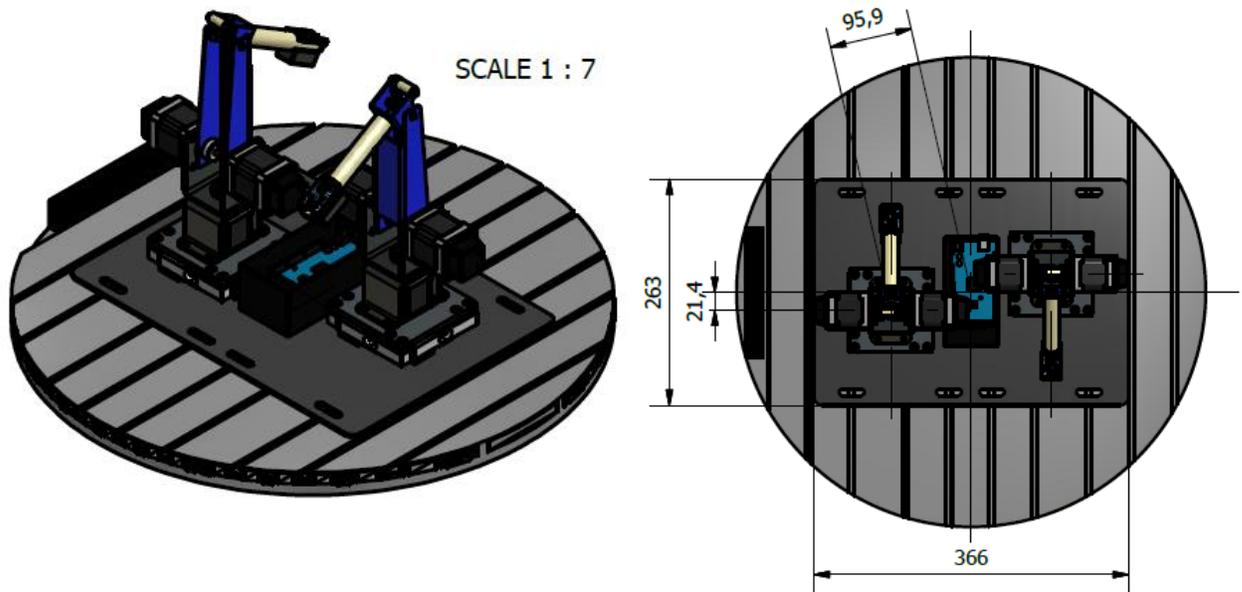
SCALE 1 : 7

95,9

263

21,4

366

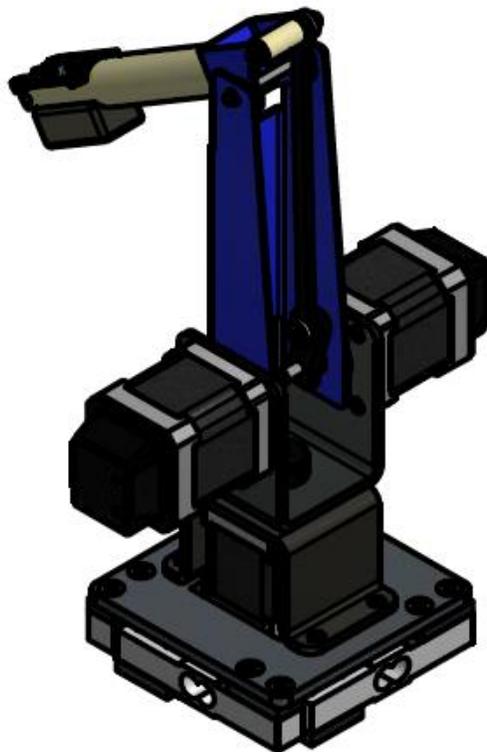Figure 1: Robotic arm manipulator setup, sketch and dimensions (units in millimeters).

Figure 2: Sketch of the robotic arm.

The final block diagram of the electronic control for the robotic manipulators is shown in Figure 3, where two independent identical controllers for each arm are depicted. The power requirements were defined as 5 V and 12 V supplies with a current capacity of 500 mA and 12 A, respectively. The final component list is detailed in Table 1 and links to additional information are provided in Appendix B.
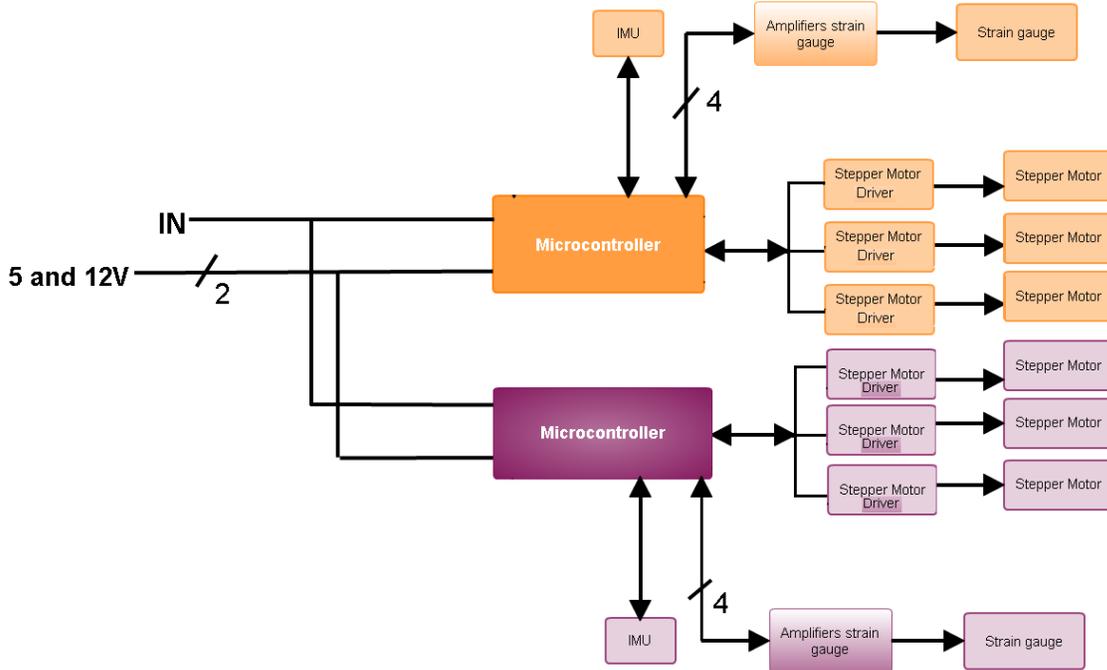

Figure 3: Updated block diagram of the electronic control system for both robotic manipulators used in the experiment.

The main controller is an *Arduino Mega Board* and several preliminary tests were made with the purchased components. Although the implemented system worked properly, the microcontroller velocity limits the possibility to create complex movement sequences and to implement a stable loop control. In the final implementation, four microcontrollers were used to acquire the sensor information separately in order decrease the processing load of the boards controlling the motors. Big easy Drivers were used as interface between the processing unit and the stepper motors, with a maximum static current of about 2 Amperes per motor.

The load cells used for the sensing at the base of each arm showed good sensitivity and acceptable precision, although they were not capable to measure the force during the impact. The cells are connected through the HX711 preamplifier modules to the controller. Encoders to monitoring the arm position were fabricated, however, they were not included in the final version due to insufficient microcontroller capacity during preliminary tests. For that reason, the arms were used in an open loop configuration.

Table 1: Electronic component list

Amount	Component
3	Arduino Mega 2560
6	Bipolar Stepper Motor 42BYGHM809
6	Big Easy Driver
2	IMU Sensor Module: Adafruit 9-DOF IMU L3GD20H + LSM303
8	Straight bar load cell TAL220
8	Load Cell Amplifier - HX711

Analytical Background

The expected observations for the experiments are justified with the analytical relations detailed in this section. Let suppose two sets of coordinate axes. Let one be the "fixed" or inertial axes, and let the other be an arbitrary frame that may be in motion (rotating system) with respect to the inertial system. The relationship between the position vector $\vec{r'}$ of the inertial system and the position vector $\vec{r}$ of the rotating system is given by:

$$\vec{r'} = \vec{r} + \vec{R}, \tag{1}$$

where the vector $\vec{R}$ locates the origin of rotating system in the fixed system.
If a point P moves there will be the relationship between velocity in the fixed system and velocity the rotatory system:

$$\left(\frac{d\vec{r}}{dt}\right)_{fixed} = \left(\frac{d\vec{r}}{dt}\right)_{rotating} + \vec{\omega} \times \vec{r} \tag{2}$$

where $\vec{\omega}$: angular velocity due to the rotation of axes and $\vec{\omega} \times \vec{r}$: velocity due to rotation of moving axes.

The Newton´s equation for inertial systems is obtained by time derivation of (2):

$$\vec{F} = m\, \vec{a}_{fixed} = m\left(\frac{d\vec{v}}{dt}\right)_{fixed}. \tag{3}$$

This equation implies:

$$\left(\frac{d\vec{v}_f}{dt}\right)_{fixed} = \left(\frac{d\vec{V}}{dt}\right)_{fixed} + \left(\frac{d\vec{v}_{Rotating}}{dt}\right)_{fixed} + \dot{\vec{\omega}} \times \vec{r} + \vec{\omega} \times \left(\frac{d\vec{r}}{dt}\right)_{fixed}$$

and we can identify that:

$$\left(\frac{d\vec{v}_{Rotating}}{dt}\right)_{fixed} = \left(\frac{d\vec{v}_{Rotating}}{dt}\right)_{Rotatory} + \vec{\omega} \times \left(\frac{d\vec{v}_{Rotating}}{dt}\right)_{fixed}$$
$$= \vec{a}_{Rotating} + \vec{\omega} \times \vec{v}_{Rotating}$$

and:

$$\vec{\omega} \times \left(\frac{d\vec{r}}{dt}\right)_{fixed} = \vec{\omega} \times \left(\frac{d\vec{r}}{dt}\right)_{Rotating} + \vec{\omega} \times (\vec{\omega} \times \vec{r}) = \vec{\omega} \times \vec{v}_{Rotating} + \vec{\omega} \times (\vec{\omega} \times \vec{r})$$

Then from (3):

$$\vec{F} = m\,\vec{a}_{fixed}$$
$$= m\left(\frac{d\vec{V}}{dt}\right)_{fixed} + m\vec{a}_{Rotating} + m\,\dot{\vec{\omega}} \times \vec{r} + m\,\vec{\omega} \times (\vec{\omega} \times \vec{r}) + 2m\,\vec{\omega} \times \vec{v}_{Rotating} \quad (4)$$

where:

$m\vec{a}_{Rotating}$:   effective force in the rotating system (the robotic arm).

$m\left(\frac{d\vec{V}}{dt}\right)_{fixed}$:   Translational (between axes) term.

$m\,\dot{\vec{\omega}} \times \vec{r}$:   Angular acceleration term.

$m\,\vec{\omega} \times (\vec{\omega} \times \vec{r})$:   Centrifugal force term (non-inertial force).

$2m\,\vec{\omega} \times \vec{v}_{Rotating}$:   Coriolis force term (non-inertial force).

From (4) we can obtain the effective force for an observer in the rotating system:

$$m\vec{a}_{Rotating}$$
$$= \vec{F} - m\left(\frac{d\vec{V}}{dt}\right)_{fixed} - m\,\dot{\vec{\omega}} \times \vec{r} - m\,\vec{\omega} \times (\vec{\omega} \times \vec{r}) - 2m\,\vec{\omega} \times \vec{v}_{Rotating} \quad (5)$$

From (5) it is straightforward that the dynamical variables will be affected by means of rotation system. When (5) is determined, we can obtain the velocity and position vectors by integrating in time:

$$\vec{v}_{eff} = \int \vec{a}_{Rotating} \; dt$$

$$\vec{r}_{eff} = \int \vec{v}_{eff} \; dt$$

In our case, we have:

$m \left(\dfrac{d\vec{V}}{dt}\right)_{fixed} = 0$ ($\vec{R}$: It does not change with time).

$\vec{\omega} = \omega \, \hat{k}$　　　　　(It does not change with time).

$\dot{\vec{\omega}} = 0$

Then:

$$m\vec{a}_{Rotating} = \vec{F} - m\,\vec{\omega}\times(\vec{\omega}\times\vec{r}) - 2m\,\vec{\omega}\times\vec{v}_{Rotating} \tag{6}$$

As a first approach to describe the theory behind the behavior of the proposed system, it will first be assumed that each arm can be treated as a particle with all its mass on its center of mass.

To calculate the angular velocity of the disk, we must first know how much spin "artificial" gravity we want to achieve. An expected number would lay in the range between 0.5g and 1g. This spin gravity value corresponds to the centripetal acceleration value of the object in the system, which is given by equation (7)

$$a_{CEN} = \omega^2 \, R \tag{7}$$

Assuming, for instance 1g:

$$a_{g,spin} = 1 \, g \tag{8}$$

Equating (7) and (8), we finally find the expression which describes the angular velocity of the disk to produce the desired value of spin gravity at a given distance.

$$\omega = \sqrt[2]{\dfrac{g}{R}} \tag{9}$$

The turntable radius is approximately 0.27m, but the arm's center of mass is at an approximate distance of 0.0935 m with respect to the center of the platform (Figure 4). Computing this value in equation (9), at g = 9.82 m/s2 gives us the angular velocity required

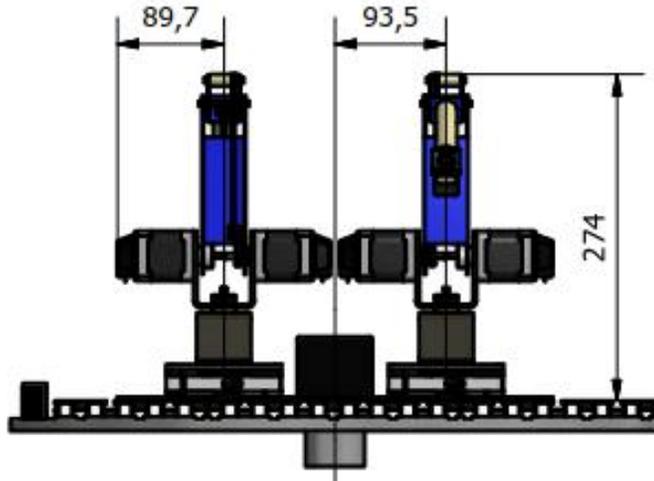$$\omega = 10.25 \frac{rad}{s} = 98 \frac{rev}{min}.$$

Figure 4. Lateral view draw of the robotic arms on the centrifuge plate (units in millimeters).

Any moving object which moves within a rotating frame of reference will be exposed to an additional inertial force called Coriolis force, which is given by equation (10). Note that the force depends on a cross product of two vectors.

$$F_{COR} = 2m \ (\omega \ x \ V_R) \tag{10}$$

where V_R is the velocity of the object with respect to the rotating frame. The cross product gives a vector which is both perpendicular to the angular velocity and the velocity of the object moving on the rotating frame. For this analysis, we are considering the velocity of the manipulator's center of mass, while the manipulator is being operated. The manipulator should do all the programmed movements within 2 seconds during the free fall, in order to have enough time to return to a safe position before impact. Assuming the center of mass moves about 5cm during the extension movement of the arm, we can calculate its average velocity.

$$V_R = \frac{\Delta X}{\Delta T} = \frac{0.05m}{2s} = 0.025 \frac{m}{s}$$

Figure 9 shows the direction of both accelerations and hence forces, due to the centrifugal and Coriolis forces. It also shows the velocity vector of the center of mass according to the proposed movement. The moving part of the assembly (not considering the motors) will have a mass of about 1kg. We may now calculate from equation (10) an expectable value of Coriolis force:

$$F_{COR} = 2 * 1kg * \left(10.25 \frac{rad}{s} * 0.025 \frac{m}{s} \right) = 0.5125 \ N$$
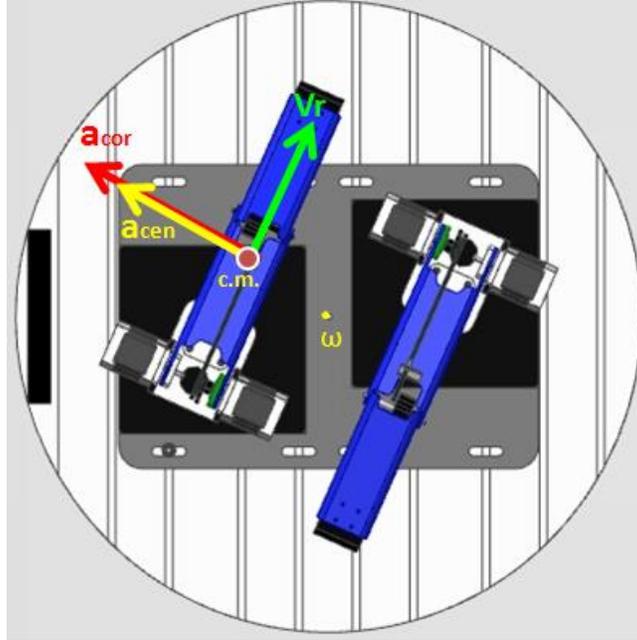$$\frac{0.5125 \ N}{9.82 \ m/s} = 52.2 \ grams$$

Figure 5. Top view of the structure with induced acceleration vectors on one arm.

Now, to measure the reactions at the base, which will be measured by the strain gauges, an equilibrium analysis must be done. Considering Figure 6, and assuming equal and opposite vertical reactions for this first approach, we get the momentum equilibrium equation as seen from this plane:

$$\sum \tau = 0 = -F_{cor} * h_{cm} - F_{cen} * h_{cm} + 2 R_Y * x_{cm} = 0 \tag{11}$$

$$R_Y = \frac{h_{cm} (F_{cor} + F_{cen})}{2 x_{cm}} \tag{12}$$

where

$$F_{cen} = m \ \omega^2 R \tag{13}$$

and

$$F_{cen} = 10.25^2 * 1 * 0.0935 \ m = 9.82 \ N$$

Finally:

$$R_Y = \frac{189.4 \ mm \ (0.52 \ N + 9.82N)}{2 * 77.5mm} = 12.6 \ N$$

Which is about the equivalent of 1.3 kg acting on the center of mass. If the manipulators position is changed, the centripetal acceleration direction will also change with respect to the arm. The effect of just the Coriolis force in this case, with no centripetal acceleration acting on this plane, would be of 0.64 N, which is about 65 grams, and still is a considerable amount

with regard to the total weight of the arm. These reactions should be sensed by the load cells, but having a better dynamical prediction.
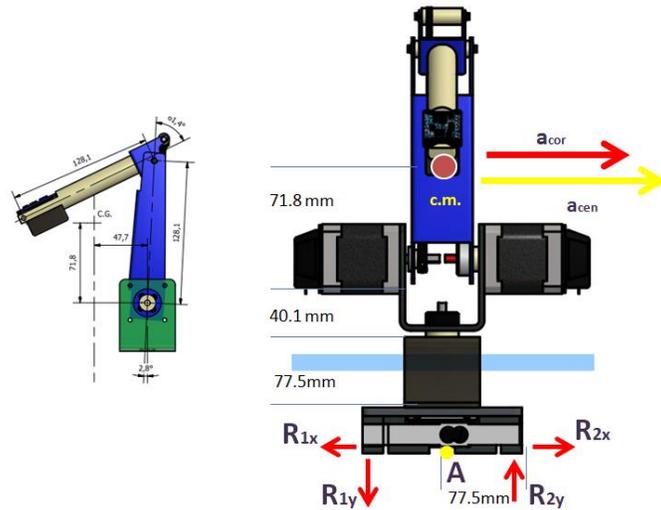

Figure 6: Expected reactions on one arm base.

III. Integration and Planning of the Experiments

An implementation of the mechanical pieces for one robotic arm were printed in ABS as preliminary verification of the design. After that, the parts were fabricated in Aluminum and Nylon; the arms were finally assembled, integrating the motor and sensors. First system tests were performed in Costa Rica to verify the functionality of the system.

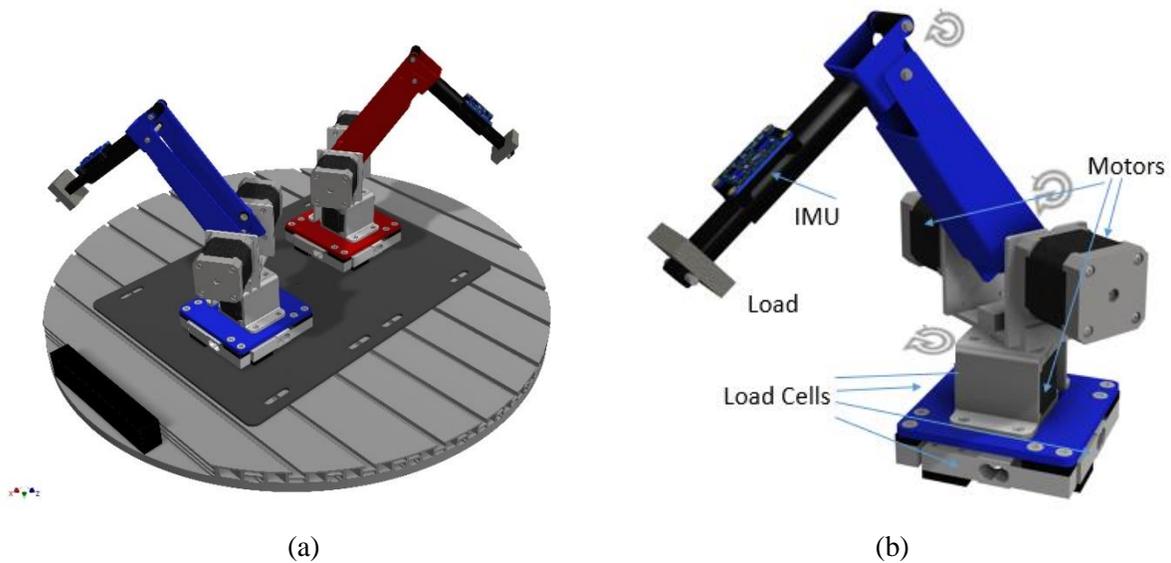(a)   (b)

Figure 7. Mechanical CAD design of the prototype: (a) complete system on the centrifuge plate. (b) Single arm detail.

The final prototype setup included two arms, symmetrically located with respect to the central point of the centrifuge plate of the capsule. Each arm was about 30 cm long and had a 50g load on its end extensor, with an approximate total weight of 1.7 kg per arm. This configuration was selected with the aim to distribute the load more evenly in the interior of the capsule. Moreover, the utilization of two arms provides redundancy to the measurements taken during the experiment and allow the establishment of a comparison basis for the cases when the two sets are collected.

Figure 7(a) shows the CAD prototype mounted on the plate, whereas Figure 7(b) shows the final configuration of one arm with sensors. The position of load cells, IMU, motors and mechanical arm load are depicted there. The first 2 DoF are controlled directly, but the third one is indirectly actuated through an extensor. The total weight of the prototype was about 5 kilogram including the electronic control.

The integration of the prototype in the capsule was performed in Bremen during the third week of November (14-20). A carefully planning of the sequence allowed the definition of a routine to exercise the 3 DoF in different directions within the available 4.7 seconds of microgravity. Note that the catapult mode was not used since the experiment required the utilization of the centrifuge. System integration within the capsule was challenging due to the mechanical considerations of the impact. The electronic system need to be reinforced and damping foams need to be included since the motors were not able to hold during the final phase of the drop. As interface between the prototype and the tower control system, trigger signals were used start the movement sequence and data acquisition. Power supply was provided with the internal battery system in the capsule.

Figure 8. Team members during the experiment integration in Bremen. From left to right: Moacir Fonseca-Becker, Renato Rimolo-Donadio, Carlos Mayorga-Espinoza, Nicole Chaves-Jiménez y Ernesto Corrales-Corrales. Photo courtesy of T. Könemann, ZARM.

The experiments were recorded with three cameras: a high-speed camera on the top of the prototype, and two lateral *GoPro* cameras. Figure 8 shows the team members at the drop tower during the integration phase. Figure 9 includes a photograph of the integrated prototype in the microgravity capsule.
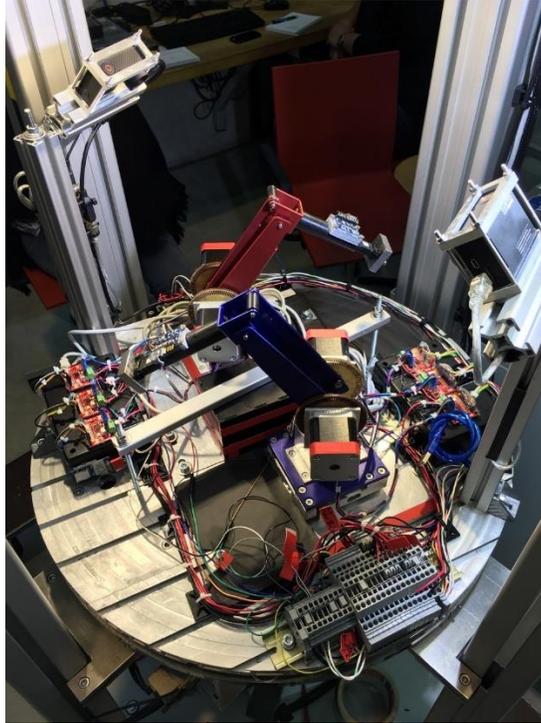

Figure 9. Integrated experiment setup. Image shows the two arms, electronic control, and side cameras integrated in the capsule.

IV. Drop Tower Experiment Series

The final stage of the project was the execution of the experiments, with four drops successfully executed. After preliminary tests on the integrated prototype, exercising the movement sequence, the four cases and the execution protocols were defined.

For all the drops, a pre- or post-repetition of the experiment was carried out with Earth gravity conditions. The same movement sequence of the arms was used to be able to stablish a comparative basis among the different experiments. The two first drops were executed with the same configuration: a centrifuge speed of 30 rpm. This, with the aim to check the repeatability of the data retrieved from the sensors, which resulted consistent once analyzed. The third drop was performed without centrifuge, in order to see the behavior without rotation. Finally, the last drop was executed with a rotation speed of 35 rpm, the maximum speed at which the motors could hold the structure and perform the programmed sequence.

Figures 10 and 11 shows the integrated experiment being loaded into the tower and a view from the control room during the execution of one experiment, respectively.

Figure 10. Drop capsule with the experiment prototype integrated in its interior (left). Inner view of the drop path within the ZARM tower (right).
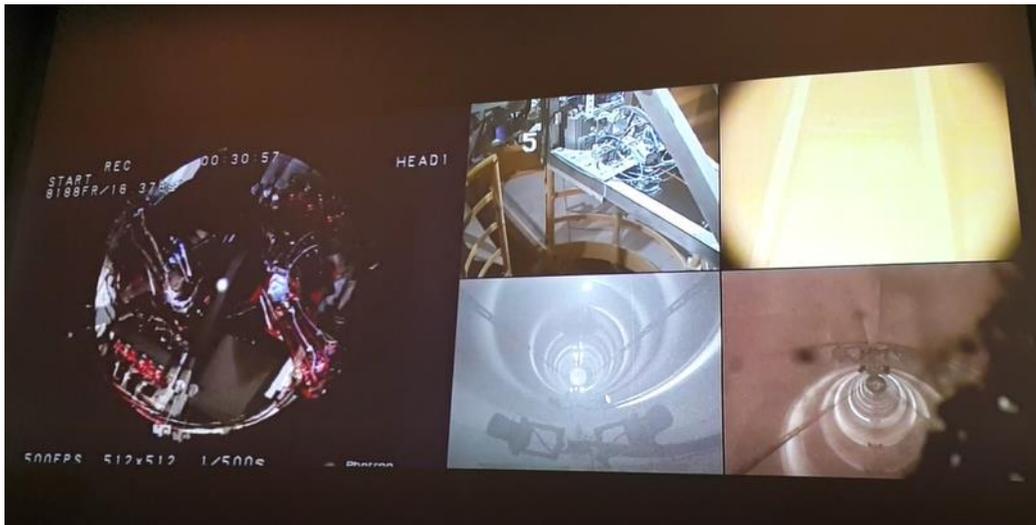

Figure 11. View from the control room at the drop tower. The prototype can be observed on the left side, from the top camera view in the capsule. The trajectory of the capsule is registered with the additional cameras (right).

The main technical results obtained from sensor acquisition were condensed in the article: *"Analysis of scaled robotic arm manipulators under microgravity conditions"*, which was accepted, as an oral presentation, to the International Aeronautical Conference (IAC) 2017 (http://www.iac2017.org/). As a contribution to that conference, the proceedings will be available at the IAF database (http://www.iafastro.org/publications/iac-papers/).

Overall, the information registered from sensors was consistent and allowed the establishment of clear trends, which are reported in the paper. Nevertheless, the accuracy was not enough for correlation of results with a theoretical model from a quantitative perspective. One of the IMUs was defective and unable to record the data, whereas the second one could register the data, but had troubles stablishing the thresholds to set the reference sensor values, probably to mechanical instabilities and the metal enclosure present during the initialization. Good quality videos could be retrieved from the experiments and a selection of them is made available through the link in Appendix C.

V. Conclusions & Outlook

The project could be ended successfully and the feasibility of studying small robotic structures in microgravity conditions using a drop tower environment has been demonstrated. To the knowledge of the team members, this is the first time that an experiment involving robotic electromechanical systems has been carried out as part of the drop tower experiment series. Although the microgravity environment can be sustained just for a few seconds (4.7 s), a carefully planning of the experiment allowed to retrieve relevant information from sensors and image devices.

The project involved the design and implementation of the double manipulator prototype and its integration on the drop tower capsule, which was a challenging task due to budget limitation, workshop and electronic component suppliers in Costa Rica, and the complexity of the electronic system itself. Nevertheless, the integration of the experiment could be completed and a series of four drops was successfully executed. In Table 2 of the Appendix A, the executed work plan is provided as a reference of the tasks completed over time. The technical results have been used to prepare a conference manuscript, which was accepted for oral presentation to the International Aeronautical Congress (IAC) 2017, in Adelaide, Australia:

N. Chaves-Jiménez, M. Fonseca-Becker, E. Corrales-Corrales, C. Mayorga-Espinoza, and R. Rimolo-Donadio, "Analysis of Scaled Robotic Arm Manipulators under Microgravity Conditions," accepted, 68th International Astronautical Congress, Adelaide, Australia, September, 2017.

Additionally, an informative article has been submitted for publication by a magazine at the Instituto Tecnológico de Costa Rica (TEC) with the aim to document the experience and to motivate the participation of Costa Rica teams in future HSTI initiatives.

For future initiatives studying robotic manipulators, it is recommended to use high quality motors and precision mechanical parts to avoid problems regarding the mechanical setup and

to ensure that the structure will support the final impact. In addition, high quality sensors, able to register more accurate data at higher speeds are also recommended. This is related also with the requirement of higher processing capacity, which might allow to execute the acquisition and control of the prototype simultaneously. The setup of the IMU needs to be also carefully planned and reviewed for future work. Its calibration might result difficult, in particular for the magnetometers due to the proximity of metallic structures.

Appendix A. Work Plan execution.

Table 2. Work plan activities and current schedule for the execution of the project (EPR 2).

	Activity	2016-17						
		Jun.	Jul.	Aug.	Set.	Oct.	Nov.	Dec. 16 - Mar. 17
1.	Submission of the first Experiment Progress Report (1 EPR, Thursday, June 16)	OK						
2.	Critical Design Review (CDR)	OK						
3.	Component purchase, fabrication and assembly of the prototype for the experiment		OK	OK	OK	OK		
4.	Submission of the second Experiment Progress Report (2 EPR: Thursday, September 15)				OK			
5.	Experiment execution and adjustment under normal gravity conditions.					OK	OK	
6.	Experiment integration: Tuesday-Friday, November 15th - 18th.						OK	
7.	Experiment Qualification: Monday, November 21st.						OK	
8.	Experiment series: Tuesday-Friday (one drop per day), November 22nd - 25th						OK	
9.	Final report and preparation of publication.							OK

Appendix B. Electronic Component External Information Links.

In this section, the updated list of electronic components used for the implementation of the robotic arms are listed, with the external links to their description.

- ➢ Arduino Mega 2560: https://www.arduino.cc/en/Main/ArduinoBoardMega2560

- ➢ Bipolar Stepper Motor 42BYGHM809:
  http://cdn.sparkfun.com/datasheets/Robotics/42BYGHM809.PDF

- ➢ Driver Motor: Big Easy Driver 11876:
  http://dlnmh9ip6v2uc.cloudfront.net/datasheets/Robotics/BigEasyDriver11876.pdf

- ➢ Adafruit 9-DOF IMU Breakout - L3GD20H + LSM303:
  https://www.adafruit.com/product/1714

- ➢ Straight bar load cell TAL220:
  https://cdn.sparkfun.com/datasheets/Sensors/ForceFlex/TAL220M4M5Update.pdf

- ➢ Load Cell Amplifier - HX711
  https://www.sparkfun.com/products/13230

Appendix C. Links to External Information.

A selection of the recorded experiments can be downloaded with the following link (file size ~600MB):
https://tecnube1-my.sharepoint.com/personal/rrimolo_itcr_ac_cr/_layouts/15/guestaccess.aspx?docid=07bf22fad4a564eaead66d75c7ba4d2ac&authkey=Aavkk8NgZL47zUeoFEyqvhg

The design CAD files of the prototype can be found here:
https://tecnube1-my.sharepoint.com/personal/rrimolo_itcr_ac_cr/_layouts/15/guestaccess.aspx?docid=01529d9a172a24bd09b03dea12e4e3f69&authkey=ATIOHgU1JRmlt3FTGMb1jaM

The informative article in InvestigaTEC will be published here:
http://revistas.tec.ac.cr/investigacion/

Temporarily, the electronic version of the magazine can be downloaded here:
https://tecnube1-my.sharepoint.com/personal/rrimolo_itcr_ac_cr/_layouts/15/guestaccess.aspx?docid=08634876ddf6e4ca69e7154f79947c5e6&authkey=AeboTBWRUDcnqdJ61w7GEcY